Available online at www.sciencedirect.com
ScienceDirect
Proceedings of the Combustion Institute 000 (2016) 1–10
Proceedings of the Combustion Institute
www.elsevier.com/locate/proci

Pressure dependence of primary soot particle size determined using thermophoretic sampling in laminar methane-air diffusion flames

Alex M. Vargas, Ömer L. Gülder*

University of Toronto Institute for Aerospace Studies, 4925 Dufferin Street, Toronto, Ontario M3H 5T6, Canada

Received 2 December 2015; accepted 26 May 2016
Available online xxx

Abstract

Optical techniques, such as the light extinction and scattering as well as the laser-induced incandescence and the spectral soot emission, have been used routinely to measure soot concentrations in atmospheric flames. Laser-induced incandescence and light scattering have been proven to measure the primary soot particle size as well in atmospheric flames; however, using these two techniques for the purpose of primary soot particle sizing in diffusion flames at elevated pressures has been found to be problematic. One of the popular methods of studying soot morphology and primary size in atmospheric flames is thermophoretic sampling followed by transmission electron microscopy analysis. A high pressure thermophoretic sampling system was built and used successfully to measure the size of primary soot particles in laminar diffusion flames of methane at pressures above atmospheric. The multi-probe sampling system was fitted inside the high-pressure combustion chamber that had been used previously for high-pressure soot formation studies. Soot samples taken at various pressures were analyzed subsequently by transmission electron microscopy to estimate the primary soot particle sizes. The soot volume fractions and soot temperatures were measured by spectral soot emission technique at the same height above the burner rim as the thermophoretic sampling. The mean primary soot particle size, measured at a constant height from the burner exit at all pressures, decreased about 35% from 2 to 10 atm whereas the soot volume fraction increased by a factor of more than 50. Experimental results of mean primary soot sizes and the corresponding soot volume fractions imply that the number of soot nuclei in soot inception region of the laminar diffusion flames must have a strong sensitivity to pressure. The higher amounts of soot are mainly determined by the increasing nucleation leading to higher primary soot particle number densities as the pressure is increased.

Keywords: Primary soot size; High-pressure flames; Thermophoretic sampling; TEM imaging of soot

1. Introduction

To achieve higher thermal efficiencies and smaller engine volumes, combustion engines are designed to operate at pressures much higher than

* Corresponding author. Tel.: +14166677721.
E-mail address: ogulder@utias.utoronto.ca, flame-utias@usa.net (Ö.L. Gülder).

http://dx.doi.org/10.1016/j.proci.2016.05.023
1540-7489 © 2016 by The Combustion Institute. Published by Elsevier Inc.

the atmospheric. One of the major pollutants emitted from the gas turbines and diesel engines is soot which forms during the combustion process when the mode of operation is non-premixed or partially-premixed, and its formation rate is significantly increased by increasing the combustion pressure [1]. Although most of the soot that formed during the combustion process in engines is oxidized within the combustion chamber, a small but important fraction escapes the oxidation process and is emitted as particulate matter from the engine exhaust. Detrimental impacts of soot on human health and climate change have been well-documented as well as its damaging effects in combustion devices. Soot particle size and morphology are crucial parameters in evaluating and appraising the influence of soot on the wellbeing of the planet and humans.

A comprehensive account of soot formation in laminar diffusion flames under elevated pressures, along with the relevant intrusive and non-intrusive measurement methods, is given in a recent review paper [1]. For soot particle size, aggregate size, fractal dimension of the aggregate, and soot concentration in atmospheric flames, laser scattering and extinction techniques have been successfully used [2–5]. Although light extinction and spectrally-resolved soot radiation have been used for soot concentration and temperature measurements at high-pressure laminar flames [6,7], light scattering to determine the soot particle size in high-pressure diffusion flames has not been demonstrated successfully yet. The laser-induced incandescence (LII) has been used at atmospheric conditions [8,9] to measure primary soot particle size and concentration with acceptable accuracy. However, there are certain issues with this technique such that the application of LII at high pressures involves several challenges that are not encountered at atmospheric pressure, in both experimental implementation and in the interpretation of the detected signals [10–12]. Ongoing refinements in the LII technique as well as those in the LII heat transfer models, which are discussed in a recent review paper [13], have improved the technique to a certain extent, but it is still not clear whether LII is capable of measuring primary soot particle size at elevated pressures [11,12,14,15]. This uncertainty necessitates the use of physical sampling approaches to complement and verify optical techniques.

As compared to the limited soot concentration measurements at pressures above atmospheric, measurements of soot morphology including the primary soot particle size at elevated pressures are scarce. Some of the information on primary soot particle size at elevated pressures have been obtained in diesel engine combustion [16,17] in which isolating the effect of pressure is challenging. Some other soot particle size measurements at elevated pressures are from shock tube experiments. Transmission electron microscopy (TEM) analysis of physically collected soot samples from shock tube experiments, in which selected fuels were being pyrolyzed, concluded that the pressure does not exhibit a marked influence on particle diameters from 25 to 50 atm [18]. On the other hand, measurements by light scattering in partially premixed burning (equivalence ratio of 5) indicated that soot formation at high pressures is characterized by particle diameters below 30 nm that decrease with increasing pressure [19].

As far as measurements in laminar diffusion flames at pressures above atmospheric are concerned, the first attempt was by Flower and Bowman [20] who investigated the primary soot size in a laminar flame stabilized on a Wolfhard–Parker burner using static-light scattering. Between atmospheric and 2.5 atm, they found that the mean particle size increases with pressure [20]. However, Flower and Bowman [20] did not keep the fuel mass flow rate constant as the pressure was increased, thus making it difficult to attribute all changes observed in soot size to pressure effects. Thomson et al. [10] used laser-induced incandescence to measure the primary soot particle size in laminar methane-air flames between 5 and 40 atm. They observed a strong influence of pressure and the primary soot particle size increased from about 25 nm at 5 atm to about 100 nm at 40 atm. However, as explained by the authors [10], what is measured with LII is the effective primary soot particle size, because the shielding effect on heat conduction between aggregated particles and the surrounding gas is neglected.

Another study that investigated the primary soot particle size on the centerline of diluted ethylene–oxygen laminar diffusion flames by thermophoretic sampling and TEM analysis concluded that soot size increases with pressure [21] from atmospheric to 8 atm. However, it should be noted that the sooting behavior of fuel-oxygen diffusion flames as compared to fuel-air ones are radically different at elevated pressures [22], and further Kim et al. [21] did not keep ethylene flow rates constant at all pressures they considered. More recently, Steinmetz et al. [23] reported an attempt in measuring the primary soot particle size by light scattering and extinction in nitrogen-diluted laminar ethylene diffusion flames at pressures from 4 to 8 atm. They argued that the flame centerline peak particle diameter is insensitive to pressure with an average size of 100–110 nm. The peak particle diameter in the flame wings grows with increasing pressure, to diameters larger than those at centerline (up to 180 nm) [23]. These diameters seem to be surprisingly large as compared to data from different devices as discussed above and could be more representative of agglomerate sizes rather than the primary soot particles casting doubt on the

Please cite this article as: A.M. Vargas, Ö.L. Gülder, Pressure dependence of primary soot particle size determined using thermophoretic sampling in laminar methane-air diffusion flames, Proceedings of the Combustion Institute (2016), http://dx.doi.org/10.1016/j.proci.2016.05.023

applicability of light scattering and extinction for sizing to high pressures.

Due to unquantified uncertainties involved in the current LII and the light scattering/extinction techniques in soot size measurements at elevated pressures, thermophoretic sampling and TEM analysis seem to be a logical avenue to investigate the influence of pressure on the primary soot size and morphology in tractable flames. Dobbins and Megaridis [24] described a thermophoretic sampling technique for soot measurements in laminar diffusion flames to provide complementary information to optical techniques. It has been used widely for atmospheric pressure flames where collected samples are analyzed by TEM, see for example [25–27]. More recently, Leschowski et al. [28] reported a design for sampling soot particles from a high-pressure laminar premixed flame by adopting the pneumatically activated sampling systems described by Dobbins and Megaridis [24] and Lee et al. [29] to high pressures.

We report measurements of mean primary soot particle size, soot volume fraction and soot temperature in methane-air diffusion flames up to a pressure of 10 atm. A multi-probe thermophoretic soot sampling system fitted into a high-pressure combustion chamber, capable of producing sooting laminar diffusion flames at elevated pressures, was used to collect the soot particle samples on TEM grids whose subsequent analysis yielded the size information as a function of pressure. A brief description of the sampling system, the disturbance of the flame by the sampling probe, and the primary soot size information as a function of pressure are presented and discussed.

2. Experimental methodology

The high-pressure combustion chamber and the laminar diffusion flame burner, along with the spectral soot emission method for temperature and soot volume fraction measurements, used in this work have been described in detail previously [22,30–36]. Only a brief description, consisting of essential details, will be given here. The combustion chamber was designed to sustain pressures up to 110 atm and its internal diameter and height are 24 and 60 cm, respectively. Optical access into the chamber is through three ports mounted at 0°, 90°, and 180° allowing line-of-sight measurements as well as 90° scattering and imaging experiments. The burner used is a circular co-flow laminar diffusion type burner which is commonly used in other similar studies. Its inner diameter at the burner rim is 3 mm and the outer diameter decreases gradually to a tapered fine edge to prevent any recirculation zones forming. The material of the burner is stainless steel and the burner tube has an insert of metal porous material to help to minimize the flow non-uniformities. The co-flow air nozzle is about 25 mm in diameter, and the air channel is also fitted with porous material for the same purpose upstream of the burner exit.

The thermophoretic sampling unit, designed to take soot samples from flames in the high pressure combustion chamber described above, consists of a circular sampling disk, a motor drive, and a programmable control system. The central part of the sampling unit is the circular sampling disk, which houses ten probe arms that extend radially outwards as shown in Figs. 1 and 2. Each sampling probe arm holds a 3 mm diameter TEM grid in a pocket that is located at the end of the probe arm. Each pocket measures 3.3 mm in diameter, has a depth of 0.5 mm, and has 2.5 mm slot that exposes the mesh of the TEM grid to the flame.

The motor drive consists of a stepper motor, a gearbox, a rotational encoder, and a homing limit switch, Fig. 1. The stepper motor's output shaft is mounted to the gearbox with a flexible coupler to prevent system vibration. The rotational encoder is mounted to the bottom of the stepper motor, to track the stepper motor displacement to within $\pm$ 0.014° during the sampling process.

The sampling velocity profile through the flame cross-section of a given height above the burner rim is controlled by the programmable control system of the sampling unit. So the residence time, i.e. the period during which the TEM grid is exposed to the flame, and the velocity of the sampling arm can be programmed as desired. For example, the probe arm can be programmed to decelerate as it enters the flame and reach a zero velocity when the TEM grid is at the desired sampling location. After the prescribed sampling time, the probe accelerates and exits the flame. Or, for cases that information averaged over the flame cross-section is desired, the probe arm can be programmed to sweep across the flame cross-section at a constant angular velocity. To start taking samples, the stepper motor drives the sampling disk at the desired velocity profile and the sampling probe arms rotate through the slot in the flame enclosure. To take samples from different heights, the flame enclosure is vertically adjusted to the desired height. After each probe arm completes the sampling process, the sampling disk is slowed down or brought to a complete stop to allow the flame to recover from the disturbance and to have a stable flame for the next sampling process. Further details of the sampling system are given in [37].

To keep measurements at different pressures tractable, fuel and air mass flow rates were kept constant at all pressures considered. The methane flow rate at all pressure levels was kept as 0.55 mg/s which corresponds to a carbon mass flow rate of 0.41 mg/s. At all pressures, a constant co-flow air mass flow of 0.34 g/s is provided.

In laminar diffusion flames stabilized in the high-pressure combustion chamber, the typical flame diameters is in the order of a few millimeters

Please cite this article as: A.M. Vargas, Ö.L. Gülder, Pressure dependence of primary soot particle size determined using thermophoretic sampling in laminar methane-air diffusion flames, Proceedings of the Combustion Institute (2016), http://dx.doi.org/10.1016/j.proci.2016.05.023

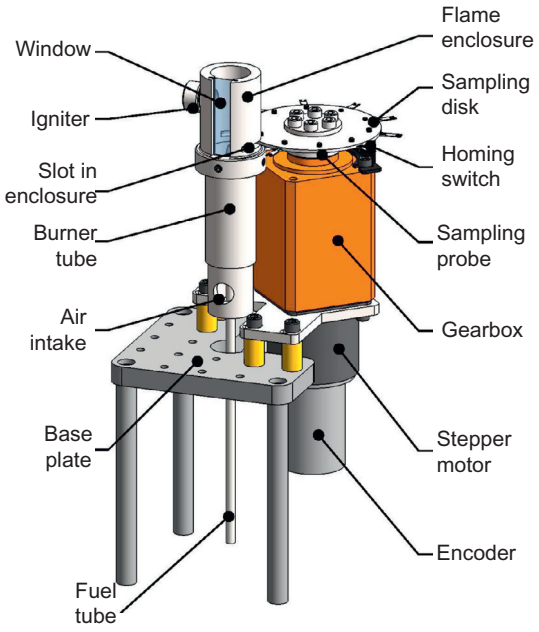

Fig. 1. Isometric view of the sampling system and the burner assembly.

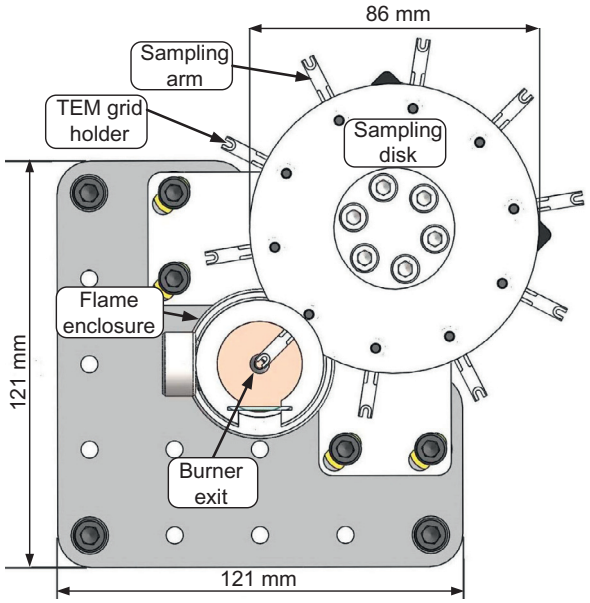

Fig. 2. Top view of the sampling disk and the burner at the center of the flame enclosure. The TEM grid holder at the end of one of the sampling probe arms is shown concentric with the burner nozzle axis.

and decreases with increasing pressure [1]. Sampling soot at a given height of the flame with a small TEM grid of 3 mm diameter at a constant angular velocity yields an averaged soot property at that flame height over the flame diameter. All measurements reported here were made at a height of 3 mm above the burner rim as it is in the soot formation dominated part of the flame and it is just before the soot yield reaches a maximum [7,30]. Soot temperatures and soot volume fractions at

Please cite this article as: A.M. Vargas, Ö.L. Gülder, Pressure dependence of primary soot particle size determined using thermophoretic sampling in laminar methane-air diffusion flames, Proceedings of the Combustion Institute (2016), http://dx.doi.org/10.1016/j.proci.2016.05.023

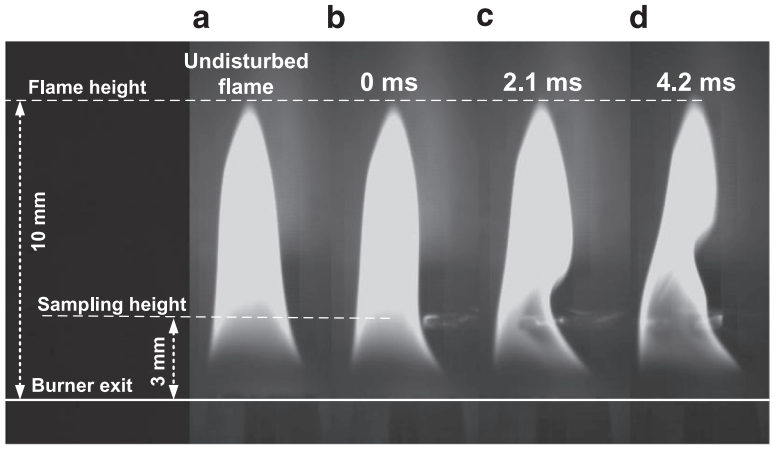

Fig. 3. Series of images depicting the disturbance of the flame by the sampling probe at 10 atm.

this height were measured using the spectral soot emission technique which was documented in detail previously [6].

The suggested practice in previous studies of soot by thermophoretic sampling and TEM analysis is that the ratio of soot covered area to grid surface area should be less than about 15% [24,29]. A trial and error approach was used to determine the suitable sampling times so that the area coverage would be less than 15% at different pressures. For the case that the sampling probe swipes through the flame at a constant angular velocity, the sampling time is defined as the time it takes for the probe to traverse the diameter of the flame at the sampling height. For the laminar diffusion flames probed in this work, sampling times of 3–8 ms gave acceptable results.

3. Results and discussion

3.1. Flow field disturbance by sampling probe

One of the major disadvantages of intrusive thermophoretic sampling is the interference created in the flow field by the insertion of the physical probe into the flame. The disturbance imposed by the sampling probe would be expected to be mostly hydrodynamic [29], and the resulting change in the flow field may have some influence on the sampling process. We captured high-speed video images of the flame flow field at 5000 frames per second using a high-frame rate camera during sampling.

A series of four flame images captured in succession displays the typical disturbance caused by the sampling probe, Fig. 3. The first image in Fig. 3, denoted as the "undisturbed flame", is that of the flame without any interference well before sampling. The condition that the edge of the thermophoretic probe is about to enter the flame is depicted as image (b) in Fig. 3. When the probe's leading edge reaches to the flame's visible boundary, the flame is slightly distorted due to presence of the probe, image (b). When the TEM grid on the probe is concentric with the flame centerline, image (c), the distortion caused by the insertion of the sampling probe looks like an indentation on the right side of the flame image. When the trailing edge of the probe is leaving the flame boundary, image (d), the flame seems to be already recovering from the distortion which has moved downstream of the sampling height. The time from the moment the probe's leading edge just entering the flame to the moment its trailing edge leaving the flame is about 4.2 ms. At 3 mm above the burner, the axial velocity along the flame centerline is about 0.5 m/s [38], whereas the linear velocity of the probe corresponding to a 4.2 ms sampling time is about 0.6 m/s which is on the same order of magnitude as the flame centerline velocity.

3.2. Primary soot particle size

Typical TEM images at 2.3, 5.4, 7.1, and 10 atm are shown in Fig. 4. Several TEM images, recorded by a TEM (Hitachi model: H-7000), processed manually using a methodology similar to those reported in the literature [25–27]. Resulting primary soot size distributions at 2.3, 5.4, 7.1, and 10 atm are shown in Fig. 5. Primary particle diameters are obtained by measuring the diameters of at least 300 particles manually in high-magnification images. Primary soot particle size histograms shown in Fig. 5 can be fitted with log-normal distribution functions (not shown) similar to size distributions reported previously at atmospheric pressures. Since all measurements were obtained at 3 mm above the burner nozzle exit and the fuel mass flow rate was

Please cite this article as: A.M. Vargas, Ö.L. Gülder, Pressure dependence of primary soot particle size determined using thermophoretic sampling in laminar methane-air diffusion flames, Proceedings of the Combustion Institute (2016), http://dx.doi.org/10.1016/j.proci.2016.05.023

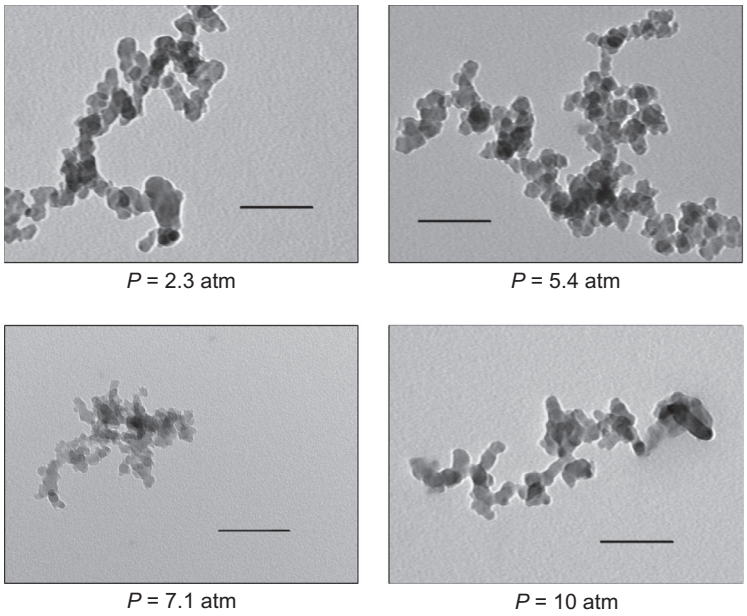

Fig. 4. Typical examples of TEM images of soot particles taken at 2.3 atm, 5.4 atm, 7.1 atm, and 10 atm. Solid bars on the images represent 100 nm.

kept constant, information at different pressure levels could be interpreted to assess the effect of pressure on primary soot particle size. The size distribution histograms shown in Fig. 5 indicate that the average primary soot particle size display a measurable decrease in diameter with increasing pressure. At 2.3 atm, the count mean diameter of primary soot particles is about 28 nm. At 5.4 atm, the diameter decreases to about 23 nm and reaches to about 17 nm at 10 atm, Fig. 5.

Soot volume fractions and soot temperatures measured by spectral soot emission at a height of 3 mm above the burner exit are shown in Fig. 6 at 5 and 10 atm. The maximum soot volume fraction at 2 atm at a height of 3 mm above the burner was measured by light extinction, Fig. 6. Considering the levels of soot volume fractions and corresponding primary soot particle sizes, it is clear that the soot number density must increase significantly with increasing pressure. The effect of pressure is to increase the number of soot nuclei which will form the primary soot particles. As the pressure increases, the overall temperature of the flame decreases because of increased radiative heat loss as a result of higher soot volume fractions, Fig. 6.

If we assume that the primary soot particles are formed by coalescence of smaller PAH clusters and subsequent surface growth, this process should be relatively slow at higher pressures so that the final primary particle size would be smaller. It should be noted that in atmospheric and in 2.3 atm flames, the size of soot particles are much smaller than the mean free path of the combustion gases. At 2.3 atm, the Knudsen number Kn, which is defined as the ratio of the mean free path of the gas to the size of the soot particle, is about 20 if we assume an average gas temperature of 1500 K. So the soot-gas system is in free-molecular regime or close to the boundary of transition regime. However, at 5.4 atm Kn number is about 10 and at 10 atm it reaches 5, which are in the transition regime and the latter condition is approaching the near-continuum regime [39]. Coalescence of particles in molecular and continuum regimes can be formulated starting from first principles; however, in the transition regime, $1 \leq \mathrm{Kn} \leq 10$, Fuchs coagulation kernel or harmonic mean of the free-molecular and slip-flow regimes kernels is generally used [40]. In their formulation of the harmonic mean coagulation kernel and subsequent analysis, Park et al. [39] show that coagulation rate decreases substantially in the transition regime from large Kn numbers to the smaller ones. Further, it is believed widely that in soot surface growth, HACA is the dominant mechanism in which the hydrogen atom plays a crucial role. However, hydrogen radical concentrations are reduced with increasing pressure, through the enhanced third-body recombination reactions, that lead to reduced soot surface growth resulting in relatively smaller primary soot particles. It can be argued that the inception rate would increase with increasing pressure due to increased chemical collision rate between PAH molecules leading to increased soot nuclei and higher primary soot

Please cite this article as: A.M. Vargas, Ö.L. Gülder, Pressure dependence of primary soot particle size determined using thermophoretic sampling in laminar methane-air diffusion flames, Proceedings of the Combustion Institute (2016), http://dx.doi.org/10.1016/j.proci.2016.05.023

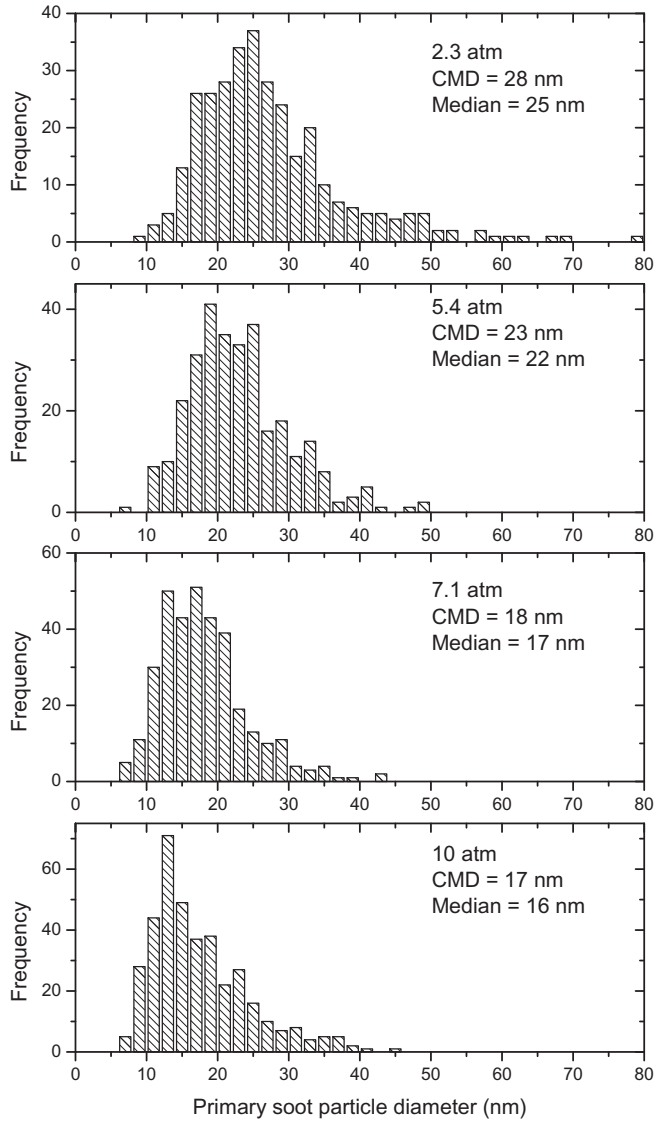

Fig. 5. Primary soot particle size distributions at 2.3, 5.4, 7.1, and 10 atm. CMD = count mean diameter.

particle number density. So higher soot volume fractions would be achieved at higher pressures by the increased primary soot particle number density in spite of decreasing primary soot particle size resulting from relatively lower coalescence and reduced surface growth rates at higher pressures. Relatively lower overall flame temperatures at higher pressures would contribute also to lower coalescence and reduced surface growth rates.

It is not possible to compare the current primary soot size measurements directly to the measurements of Flower and Bowman [20], Thomson et al. [10], Kim et al. [21], or Steinmetz et al. [23]. As discussed in the Introduction section, Flower and Bowman [20] and Kim et al. [21] did not keep mass flow rates of fuel constant in their experiments as the pressure was changed, thus, it is not possible to attribute the changes they observed in the primary soot particle size to pressure only. Thomson et al. [10] indicated that the primary soot particle size measured by LII at elevated pressures does not correspond to the actual primary soot size but to an effective diameter because the shielding effect on heat conduction between aggregated particles and the surrounding gas is not taken into account. For this reason, the effective particle diameter is a function of the primary particle diameter and the aggregate morphology. As a result it is not possible to

Please cite this article as: A.M. Vargas, Ö.L. Gülder, Pressure dependence of primary soot particle size determined using thermophoretic sampling in laminar methane-air diffusion flames, Proceedings of the Combustion Institute (2016), http://dx.doi.org/10.1016/j.proci.2016.05.023

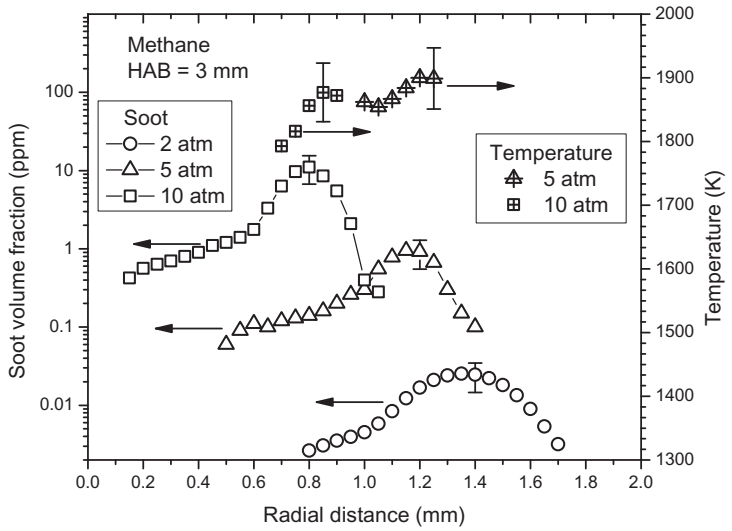

Fig. 6. Soot volume fractions at 2, 5, and 10 atm and soot temperatures at 5 and 10 atm. Error bars correspond to measurement uncertainties discussed previously, see for example [7].

know whether a change in measured effective particle diameter is caused by a variation of the primary soot particle size, aggregate characteristics, or both [10]. In a recent paper, Steinmetz et al. [41] reported measurements of the average weighted primary particle diameter and average primary particle diameter at pressures from 4 to 16 atm using light scattering. They reported an increase in both particle diameters with increasing pressure. However, similar to the conclusion given by Thomson et al. [10], they indicated that what is measured is an intermediate average diameter between that of the primary particles and the soot aggregates [41].

The current study is the first thermophoretic sampling attempt, to the authors' knowledge, in tractable high-pressure laminar diffusion flames. It should be noted, however, that the current measurements of the mean primary soot particle size at pressures above atmospheric are not radially resolved at the selected sampling height above the burner exit. These measurements of primary soot particle size are averaged values over the flame cross-sectional area at 3 mm height above the burner exit because of the constraints imposed by the diameter of the laminar diffusion flames at elevated pressures and the size of the sampling grids. There is evidence, at least at atmospheric conditions, that the primary soot particle diameters could differ from the flame centerline to the flame wings [42]. Along with soot volume fraction and soot temperature measurements, the current mean particle size information would be useful for numerical models as well as demonstrating the behavior of primary soot size with pressure in well-controlled laminar diffusion flames. Similar to those reported previously for TEM imaging to measure primary soot particle size [26], the experimental uncertainty was estimated to be within 15% (95% confidence interval). It is not trivial to assess the effect of parameters such as particle number density, temperature at the sampling location, and the Knudsen number on sampling and the uncertainty introduced by them. It was assumed that, to a first approximation, the thermophoretic force and velocity do not change significantly with the Knudsen number in the transition regime, see for example, Talbot et al. [43].

3.3. Effect of sampling time on soot size measurements

A series of sampling experiments was repeated with various sampling times to assess the influence of sampling time on primary soot particle size measurements. Resulting mean soot diameters evaluated from samples collected with various sampling times are shown in Fig. 7 at 2.3, 4, 5.4, 7.1 and 10 atm. The estimated primary soot particle diameters and their overall behavior with pressure did not change significantly by changing the sampling time from 4.6 ms to 5.4 or to 7.6 ms. The spread of the primary soot particle size distribution, represented by error bars in Fig. 7, corresponds to two standard deviations of the size distribution. The variance in primary particle size distributions decreased generally as pressure increased.

4. Conclusions

A high pressure thermophoretic sampling system was designed, built, and used successfully to measure the size of primary soot particles in laminar diffusion flames of methane at pressures above

Please cite this article as: A.M. Vargas, Ö.L. Gülder, Pressure dependence of primary soot particle size determined using thermophoretic sampling in laminar methane-air diffusion flames, Proceedings of the Combustion Institute (2016), http://dx.doi.org/10.1016/j.proci.2016.05.023

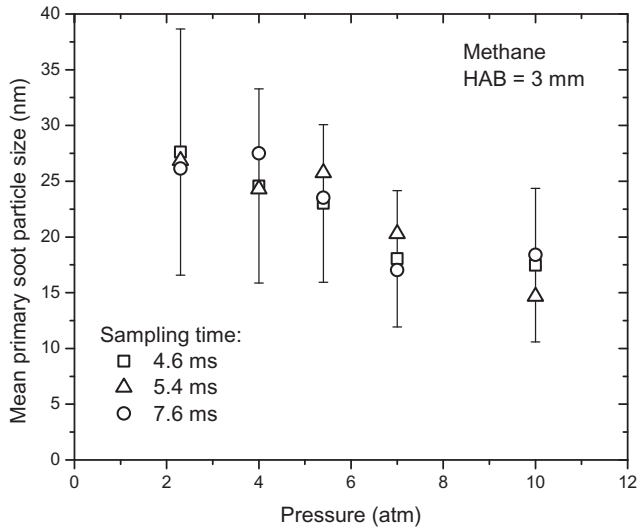

Fig. 7. Variation of the count mean particle size with pressure at various sampling times. The error bars shown for 4.6 ms sampling time correspond to two standard deviations of the size distribution. Similar variances are obtained for longer sampling times; however, they are not shown in the plot for clarity.

atmospheric. Soot samples taken at various pressures from laminar diffusion flames of methane were analyzed by transmission electron microscopy to estimate the primary soot particle sizes. The mean soot primary particle size, measured at a constant height of 3 mm from the burner exit at all pressures, decreased about 35% from 2 to 10 atm. At the sampling height of 3 mm, the maximum soot volume fraction increased from a fraction of one ppm at 2 atm to 1 ppm at 5 atm and to about 10 ppm at 10 atm. Mean primary soot sizes and the corresponding soot volume fractions indicate that the soot number density in the soot formation dominated portion of the laminar diffusion flames increases with increasing pressure. Measured primary soot sizes and soot volume fractions at elevated pressures indicate that the effect of pressure is to increase the number of soot nuclei which will grow to primary soot particles. It was argued that the decrease in primary soot size with increasing pressure is due to two reasons: (a) a reduction in the rate of coalescence with increasing pressure as a result of the Knudsen number changing from about 20 at 2 atm to about 5 at 10 atm within the transition regime, and (b) a reduction in the hydrogen radical concentration with increasing pressure leading to reduced surface growth through the HACA mechanism.

Acknowledgments

The authors thank the Natural Sciences and Engineering Research Council of Canada for the support provided for this work through discovery (251116–2012) and strategic project (STPGP 430362–12) grants.

References

[1] A.E. Karataş, Ö.L. Gülder, *Prog. Energy Combust. Sci.* 38 (2012) 818–845.
[2] C.M. Sorensen, J. Cai, N. Lu, *Langmuir* 8 (1992) 2064–2069.
[3] C.M. Sorensen, J. Cai, N. Lu, *Appl. Opt.* 31 (30) (1992) 6547–6557.
[4] R. Puri, T.F. Richardson, R.J. Santoro, R.A. Dobbins, *Combust. Flame* 92 (1993) 320–333.
[5] Ü.Ö. Köylü, G.M. Faeth, *J. Heat Transf.* 118 (2) (1996) 415–421.
[6] D.R. Snelling, K.A. Thomson, G.J. Smallwood, Ö.L. Gülder, E.J. Weckman, R.A. Fraser, *AIAA J.* 40 (2002) 1789–1795.
[7] K.A. Thomson, Ö.L. Gülder, E.J. Weckman, R.A. Fraser, G.J. Smallwood, D.R. Snelling, *Combust. Flame* 140 (2005) 222–232.
[8] D.R. Snelling, F. Liu, G.J. Smallwood, Ö.L. Gülder, *Combust. Flame* 136 (2004) 180–190.
[9] D.R. Snelling, G.J. Smallwood, F. Liu, Ö.L. Gülder, *Appl. Opt.* 44 (31) (2005) 6773–6785.
[10] K.A. Thomson, D.R. Snelling, G.J. Smallwood, F. Liu, *Appl. Phys. B: Lasers Opt.* 83 (2006) 469–475.
[11] M. Leschowski, T. Dreier, C. Schulz, *Z. Phys. Chem.* 229 (2015) 781–805.
[12] E. Cenker, G. Bruneaux, T. Dreier, C. Schulz, *Appl. Phys. B: Lasers Opt.* 119 (2015) 745–763.
[13] H. Michelsen, C. Schulz, G. Smallwood, S. Will, *Prog. Energy Combust. Sci.* 51 (2015) 2–48.
[14] M. Hofmann, B.F. Kock, T. Dreier, H. Jander, C. Schulz, *Appl. Phys. B: Lasers Opt.* 90 (3–4) (2008) 629–639.
[15] M. Charwath, R. Suntz, H. Bockhorn, *Appl. Phys. B: Lasers Opt.* 104 (2011) 427–438.

Please cite this article as: A.M. Vargas, Ö.L. Gülder, Pressure dependence of primary soot particle size determined using thermophoretic sampling in laminar methane-air diffusion flames, Proceedings of the Combustion Institute (2016), http://dx.doi.org/10.1016/j.proci.2016.05.023

[16] R. Ryser, T. Gerber, T. Dreier, *Combust. Flame* 156 (2009) 120–129.
[17] R. Zhan, S. Kook, *Environ. Sci. Technol.* 48 (2014) 8243–8250.
[18] S. Baurle, Y. Karasevich, S. Slavov, et al., *Proc. Combust. Inst.* 25 (1994) 627–634.
[19] H. Kellerer, A. Moller, H.-J. Bauer, S. Wittig, *Combust. Sci. Technol.* 113–114 (1996) 67–80.
[20] W.L. Flower, C.T. Bowman, *Proc. Combust. Inst.* 20 (1984) 1035–1044.
[21] C.H. Kim, F. Xu, G.M. Faeth, *Combust. Flame* 152 (3) (2008) 301–313.
[22] P.H. Joo, M.R.J. Charest, C.P.T. Groth, Ö.L. Gülder, *Combust. Flame* 160 (2013) 1990–1998.
[23] S.A. Steinmetz, T. Fang, W.L. Roberts, in: European Combustion Meeting, Poster No. 53, 2013, University of Lund, 2013.
[24] R.A. Dobbins, C.M. Megaridis, *Langmuir* 3 (1987) 254–259.
[25] Ü.Ö. Köylü, C.S. McEnally, D.E. Rosner, L.D. Pfefferle, *Combust. Flame* 110 (1997) 494–507.
[26] B. Hu, B. Yang, Ü.Ö. Köylü, *Combust. Flame* 134 (2003) 93–106.
[27] B. Hu, Ü.Ö. Köylü, *Aerosol Sci. Technol.* 38 (2004) 1009–1018.
[28] M. Leschowski, T. Dreier, C. Schulz, *Rev. Sci. Instrum.* 85 (2014) 045103.
[29] J. Lee, I. Altman, M. Choi, *J. Aerosol Sci.* 39 (5) (2008) 418–431.
[30] H.I. Joo, Ö.L. Gülder, *Proc. Combust. Inst.* 32 (2009) 769–775.
[31] Ö.L. Gülder, G. Intasopa, H.I. Joo, P.M. Mandatori, D.S. Bento, M.E. Vaillancourt, *Combust. Flame* 158 (2011) 2037–2044.
[32] H.I. Joo, Ö.L. Gülder, *Combust. Flame* 158 (2011) 416–422.
[33] P.M. Mandatori, Ö.L. Gülder, *Proc. Combust. Inst.* 33 (2011) 577–584.
[34] P.H. Joo, Ö.L. Gülder, *Energy Fuels* 26 (2012) 5462–5467.
[35] A.E. Karataş, G. Intasopa, Ö.L. Gülder, *Combust. Flame* 160 (2013) 1650–1656.
[36] F. Liu, A.E. Karataş, Ö.L. Gülder, M. Gu, *Combust. Flame* 162 (5) (2015) 2231–2247.
[37] A.M. Vargas, Ö.L. Gülder, *Rev. Sci. Instrum.* 87 (5) (2016) 055101.
[38] M.R.J. Charest, H.I. Joo, Ö.L. Gülder, C.P.T. Groth, *Proc. Combust. Inst.* 33 (1) (2011) 549–557.
[39] S.H. Park, K.W. Lee, E. Otto, H. Fissan, *J. Aerosol Sci.* 30 (1999) 3–16.
[40] R.I.A. Patterson, J. Singh, M. Balthasar, M. Kraft, W. Wagner, *Combust. Flame* 145 (2006) 638–642.
[41] S.A. Steinmetz, T. Fang, W.L. Roberts, *Combust. Flame* 169 (2016) 85–93.
[42] M. Kholghy, M. Saffaripour, C. Yip, M.J. Thomson, *Combust. Flame* 160 (2013) 2119–2130.
[43] L. Talbot, R.K. Cheng, R.W. Schefer, D.R. Willis, *J. Fluid Mech.* 101 (1980) 737–758.

Please cite this article as: A.M. Vargas, Ö.L. Gülder, Pressure dependence of primary soot particle size determined using thermophoretic sampling in laminar methane-air diffusion flames, Proceedings of the Combustion Institute (2016), http://dx.doi.org/10.1016/j.proci.2016.05.023